Science in China Series B: Chemistry

Springer

www.scichina.com
chem.scichina.com
www.springerlink.com

Comparative proteomics analysis of lanthanum citrate complex-induced apoptosis in HeLa cells

SHEN LiMing, LIU Qiong & NI JiaZuan†

College of Life Sciences, Shenzhen University, Shenzhen 518060, China

In a previous study, the lanthanum citrate complex ($[LaCit_2]^{3-}$) has been found to induce apoptosis in the human HeLa cervical cancer cell line. To clarify the mechanism, we carried out comparative proteomics analysis between treated and control cells. Differentially expressed proteins were separated electrophoretically and identified by MALDI-TOF/TOF tandem mass spectrometry. There were profound changes in 14 proteins related to mitochondrial function and oxidative stress, suggesting that mitochondrial dysfunction plays a key role in $[LaCit_2]^{3-}$-induced apoptosis. This was confirmed by a decrease in the mitochondrial transmembrane potential, and increases in cytochrome c release and reactive oxygen species generation in $[LaCit_2]^{3-}$-treated cells. Western blotting analyses show that $[LaCit_2]^{3-}$-induced apoptosis was accompanied by the activation of caspase-9 and the specific proteolytic cleavage of PARP, leading to an increase in the proapoptotic protein Bax and a decrease in the antiapoptotic protein Bcl-2. These results suggest that $[LaCit_2]^{3-}$ induced the apoptosis of HeLa cells through oxidative stress mediated pathway involving MT participation.

lanthanum citrate complex, HeLa cells, proteomics

1 Introduction

Effects of La^{3+} on cell proliferation and apoptosis have been studied extensively[1−4]. Whether lanthanides promote cell proliferation or induce cell apoptosis depends on their concentrations and the types of cancer cells being studied. Lanthanum citrate was reported to inhibit the growth of human lung cancer PG cell line dose-dependently, but it did not affect human gastric cancer BGC-823 cells or human embryo diploid fibroblast cells. It arrested PG cells in the G1 phase and inhibited DNA synthesis, which is consistent with the inhibition of cell proliferation[5]. Up to date, a redox-active gadolinium texaphyrin complex has entered phase Ⅲ clinical trials for the treatment of patients with brain metastases of non-small cell lung carcinomas[6]. In addition, it was also proposed that lanthanides might induce apoptosis via mitochondrial (MT) pathways[7−9] and it appears likely that reactive oxygen species (ROS) are involved in the mechanism[8,9]. La^{3+} induced cell proliferation and apoptosis in a manner compatible with a p53-related mechanism in NIH 3T3 cells via an ERK-mediated signaling cascade induced by a metal-sensing mechanism[2,10]. Lanthanum compounds also interact with DNA by mechanisms involving intercalation or coordinative binding[11,12].

In our previous work, a dose-dependent effect of $[LaCit_2]^{3-}$ was studied on the growth and viability of different cancer cell lines[13]. $[LaCit_2]^{3-}$ inhibited the growth of different cancer cell lines at high concentrations, but no significant inhibition was observed at low concentrations. Additionally, the effect of $[LaCit_2]^{3-}$ on cell growth also depends on the type of cancer cells. The most potent cytotoxicity of $[LaCit_2]^{3-}$ was observed in

Received August 15, 2009; accepted September 3, 2009
doi: 10.1007/s11426-009-0272-z
†Corresponding author (email: jzni@szu.edu.cn)
Supported by the National Natural Science Foundation of China (Grant No. 20637010) and the Shenzhen Bureau of Science, Technology and Information

HeLa cells, while it had relatively lower cytotoxicity toward human breast cancer (MCF 7), prostate cancer (PC-3), lung cancer (PG) and hepatocellular carcinoma (HepG2) cell lines.

In this study, $[LaCit_2]^{3-}$-induced apoptosis in HeLa cells was explored using a proteomic approach. Using two-dimensional gel electrophoresis (2-DE) on proteins extracted from control and $[LaCit_2]^{3-}$-treated cells, differentially expressed proteins were observed and identified by matrix-assisted laser desorption/ionization time-of-flight tandem mass spectrometry (MALDI-TOF/TOF MS). Confirmed by the results of Western blotting analysis, measurements of $\Delta\Psi_m$, cytochrome c (cyt-c) release and intracellular H_2O_2 level, we conclude that $[LaCit_2]^{3-}$ induces apoptosis by activating intrinsic apoptotic pathways.

2 Materials and methods

2.1 Materials

The human HeLa cervical epithelial cell line was purchased from the Shanghai Institute of Biochemistry and Cell Biology, Chinese Academy of Sciences. $[LaCit_2]^{3-}$ solution was prepared as described previously[13] from lanthanum oxide (purity >99.9%, Yuelong New Materials Co., Ltd., Shanghai, China) and citric acid (BBI, Canada). All other reagents were obtained from GE Healthcare (Yian Plaza, Guangzhou, China), unless otherwise noted.

2.2 Cell culture

The cells were cultured in RPMI-1640 medium plus 10% fetal bovine serum (FBS) (Hyclone, Logan, UT, USA), 100 U·mL penicillin and 100 μg·mL streptomycin (Merck & Co., Inc, Whitehouse Station, NJ, USA). The cells were maintained in a humidified incubator in 95% air and 5% CO_2 at 37℃. When the cells reached 80% confluence, they were harvested and plated for either subsequent passages or drug treatments. For the treated samples, the medium was removed and fresh FBS-free RPMI-1640 medium containing 0.15 mmol·L^{-1} $[LaCit_2]^{3-}$ was added.

2.3 Proteome analysis

After treatment with 0.15 mmol·L^{-1} $[LaCit_2]^{3-}$ for 24 h, the cells were harvested and the proteins were extracted as described previously[14]. 2-DE was performed using IPGphor isoelectric focusing (IEF) and electrophoresis units (GE Healthcare)[14]. Briefly, whole cell protein lysates (150 μg for analysis gels and 800 μg for preparative gels) were mixed with rehydration solution to a final volume of 450 μL. Precast 24 cm immobilized pH gradient (IPG) strips were rehydrated for 12 h at 30 V, and IEF was performed for a total of 75000 Vh. After the first dimensional run, the proteins were reduced in equilibration buffer and alkylated for 15 min in the same buffer containing 135 mmol·L^{-1} iodoacetamide instead of DTT. Proteins were then separated in the second dimensional gel made from 12.5% SDS-polyacrylamide using the Ettan DALT*six* Electrophoresis Unit. The second dimensional gels for analysis were stained with silver nitrate and the gels for mass spectrometry were stained with Coomassie brilliant blue G-250. The gels were scanned with ProXPRESS 2D imaging system (Perkin-Elmer Inc., Waltham, MA, USA) and analyzed with Image Master 2D Elite software (GE Healthcare). Only those spots that changed consistently in three replicates and significantly (more than 2.0-fold) were selected for the analysis with MS. These spots were excised and the gel pieces were subjected to in-gel digestion with trypsin followed by polypeptide analysis using MALDI-MS and PMF[14]. MASCOT was used in database searching for protein identification by MS data in the NCBI database (http://www.ncbi.nlm.nih.gov/).

2.4 Measurement of MT transmembrane potential and oxidative stress

Flow cytometry was used for the analysis of $\Delta\Psi_m$ and generation of H_2O_2. Briefly, after $[LaCit_2]^{3-}$ treatment, the cells were incubated with 5 mg·L JC-1 (Beyotime Biotech, Jiangsu, China) or 10 μmol·L^{-1} DCFH-DA (Beyotime Biotech). Flow cytometry was performed using a Beckman Coulter Altra flow cytometer equipped with a single 488 nm argon laser. A minimum of 10,000 cells per sample was acquired and analyzed using WinMDI V2.8 software.

2.5 Detection of cyt-c release from the mitochondria

Cells were grown on 35 mm glass bottom culture dish (MatTek Corporation, German) and treated with 0.15 mmol·L^{-1} $[LaCit_2]^{3-}$ for 6 or 16 h as described above. Immunocytochemistry was performed using primary antibody to cyt-c and a secondary anti-mouse IgG antibody conjugated with Cy3 (Beyotime Biotech), and processed as described in the manufacturer's protocol and ref. [8].

2.6 Western blotting

Western blotting was performed as described previously[14] using primary antibodies (Abs) against Bcl-2 (from Santa Cruz Biotechnology, Santa Cruz, CA, USA), Bax (Santa Cruz), caspase-9 (Santa Cruz), PARP (Beyotime Biotech), SOD1 (BIOS, Beijing, China), VDAC1 (Santa Cruz), VDAC2 (Santa Cruz), Nm23 (BIOS) and eEF2 (from Abzoom, Dallas, TX, USA) at optimized dilutions. GAPDH (Santa Cruz) was used for the normalization of each protein to ensure equal protein loading.

3 Results and discussion

3.1 MT dysfunction is a key event in the apoptosis induced by $[LaCit_2]^{3-}$

The proteomes of control and $[LaCit_2]^{3-}$-treated cells were analyzed by 2-DE. Representative gel images are shown in Figure 1. By applying a threshold of 2-fold variation, 14 spots were identified as differentially expressed after $[LaCit_2]^{3-}$ treatment. Table 1 lists the differentially expressed proteins identified by peptide mass fingerprinting (PMF). The first group was proteins involved in apoptosis and cell proliferation. Expressions of human nucleoside diphosphate kinase B, nucleophosmin (NPM), S100 calcium binding protein A11 (S100-A11) were downregulated, whereas the prohibitin (PHB) was upregulated. The second group of proteins was related to stress response and redox activity. Heat shock 70-kDa protein 9 precursor, heat shock protein beta-8 (HspB8) and superoxide dismutase 1 (SOD1) were decreased, whereas the level of probable bifunctional methylenetetrahydrofolate (MTHFD2**)** was increased. Another group of proteins was related to translation and protein degradation, including the downregulation of eukaryotic translation elongation factor 2 (eFF2), ribosomal protein (RPLP0), calreticulin precursor variant and far upstream element (FUSE) binding protein 1, isoform CRA_b and the upregulation of proteasome beta 3 subunit. Several representative proteins were selected from each group to be further confirmed by western blot analysis, while others remained to be confirmed later.

The $\Delta\Psi_m$ and H_2O_2 levels were measured in relation to the proteomic changes of MT proteins and oxidative stress. The experimental results show that $[LaCit_2]^{3-}$ treatment resulted in a decrease in $\Delta\Psi_m$ (Figure 2(a)) and the generation of H_2O_2 (Figure 2(b)). In addition, apoptotic stimuli generally induce the opening of the membrane permeability transition (MPT) pores and swelling followed by release of proapoptotic proteins from the MT intermembranous space[15,16]. We observed the cyt-c

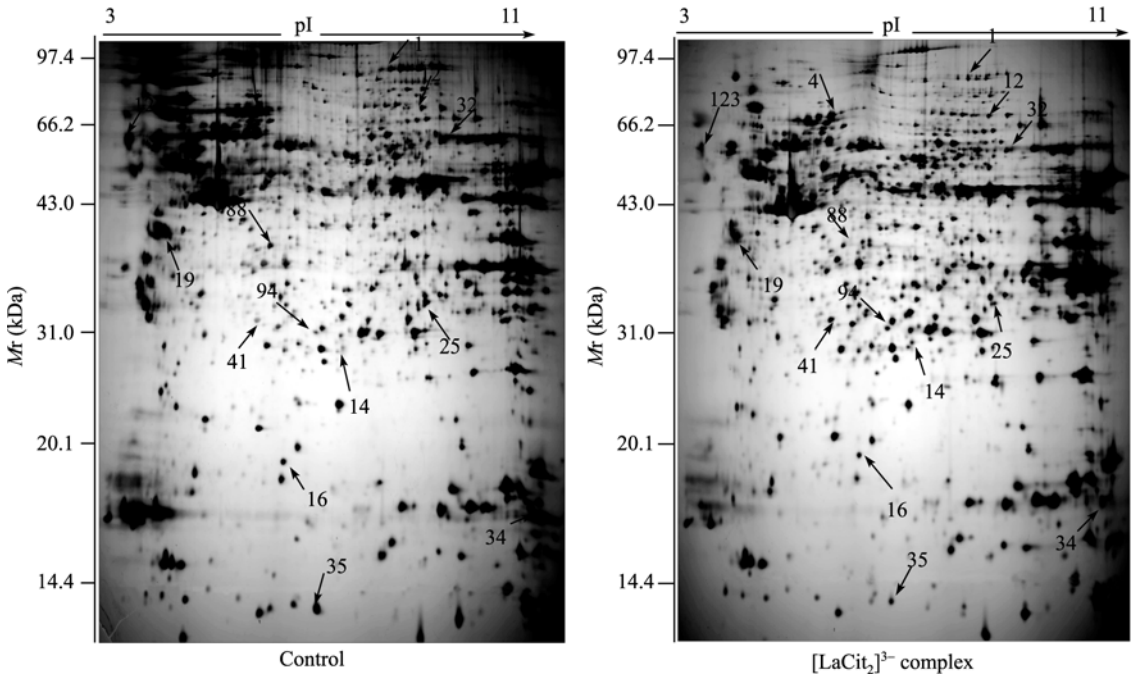

Figure 1 Two-dimensional gel electrophoresis (2D-GE) images of control and $[LaCit_2]^{3-}$-treated cells. The arrows indicate those proteins whose expressions were altered and identified by peptide mass fingerprinting (PMF). The numbers are correlated with that spot number listed in Table 1.

Table 1 Proteins identified by mass spectrometry and their alterations in the proteome after $[LaCit_2]^{3-}$ treatment (0.15 mmol·L^{-1} for 24 h)

Spot no.	Protein ID	NCBI accession no.	MW (kDa)/pI	Reported function	Expression level [a)]	Peptides matched [b)]
1	Eukaryotic translation elongation factor 2 (eEF2)	4503483	95.3/6.41	Translation	–	15
4	Heat shock 70 kDa protein 9 precursor	24234688	73.6/5.87	response to stress	–	6
12	Far upstream element (FUSE) binding protein 1, isoform CRA_b	119626762	68.7/7.18	RNA folding	–	10
14	Proteasome beta 3 subunit	22538465	23.2/6.14	protein degradation	+	9
16	Superoxide dismutase 1, soluble (SOD1)	4507149	16.1/5.7	oxidation reduction	–	6
19	Nucleolar phospho-protein B23, numatrin (NPM)	18314408	32.5/4.59	anti-apoptosis	–	9
25	HCG1785879	119602242	10.8/11.3121.	unclear	–	6
32	Heat shock protein beta-8 (HspB8)	5901655	5/5.0	response to stress	–	5
34	Human nucleoside diphosphate kinase B complexed (Nm23)	1421609	17.1/8.55	apoptosis	–	8
35	S100 calcium binding protein A11 (S100-A11)	5032057	11.8/6.56	cell proliferation	–	6
41	Prohibitin (PHB)	4505773	29.8/5.57	apoptosis	+	7
88	Ribosomal protein, large, P0 (RPLP0)	12654583	34.2/5.42	translation	–	9
94	Probable bifunctional methylenetetra -hydrofolate dehydrogenase/cyclohy -drolase2(MTHFD2L)	10434969	25.8/8.54	oxidation reduction	+	6
123	Calreticulin precursor variant	62897681	46.9/4.3	protein folding	–	10

a) Expression levels in $[LaCit_2]^{3-}$-treated HeLa cells at 24 h compared with the control (+, increase; –, decrease); b) peptides matched: unique peptides identified by peptide mass fingerprinting.

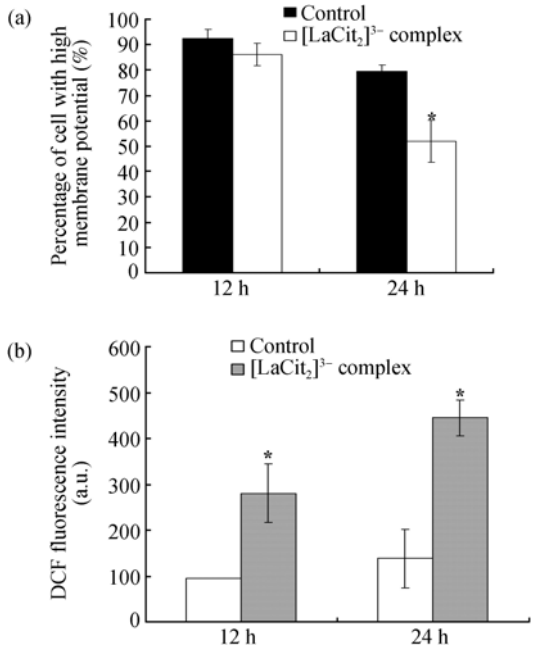

Figure 2 Mitochondrial membrane potential changes ($\Delta\Psi_m$) and $[LaCit_2]^{3-}$-induced generation of H_2O_2 in HeLa cells. (a) Percentages of cells with high $\Delta\Psi_m$. Each value represents the mean ± S.D. of three separate determinations (*$P < 0.05$ compared with the control.) (b) HeLa cells were pretreated with 0.15 mmol·L^{-1} $[LaCit_2]^{3-}$ in FBS-free medium for 24 h and incubated with 10 mmol·L^{-1} DCFH-DA for 30 min at 37℃. The fluorescence intensity was measured using flow cytometry (*$P < 0.05$).

release from the MT (Figure 3), the activation of caspase-9 and the 89 kDa cleaved form of PARP (Figure 4(a)). Moreover, the expression level of the proapoptotic protein Bax was increased whereas the antiapoptotic protein Bcl-2 was decreased (Figure 4(a)). Most signals that control the survival of mammalian cells modulate the activity of the Bcl-2 family of proteins, which are well-characterized regulators of the MT pathway of apoptosis. The intracellular balance of Bax and Bcl-2 could decide the cell fate: death or survival[17]. In addition, here we found that caspases acted as downstream activators of $[LaCit_2]^{3-}$-induced apoptosis and that MT permeabilization was mediated by the regulation of the Bcl-2 family proteins in $[LaCit_2]^{3-}$-treated HeLa cells. These results suggest that $[LaCit_2]^{3-}$-induced stress leads to MT dysfunction, which in turn induces cell apoptosis as well as inhibits protein synthesis.

As described above, the mitochondria respond to an apoptotic signal by opening the PTP. This is composed of the VDAC, OMM (Outer Mitochondrial Membrane), the adenine nucleotide translocase (ANT) and cyclophilin D. Recent studies involving both down- and overexpression clearly indicate that the expression level of VDAC is a critical element in cell life and death and

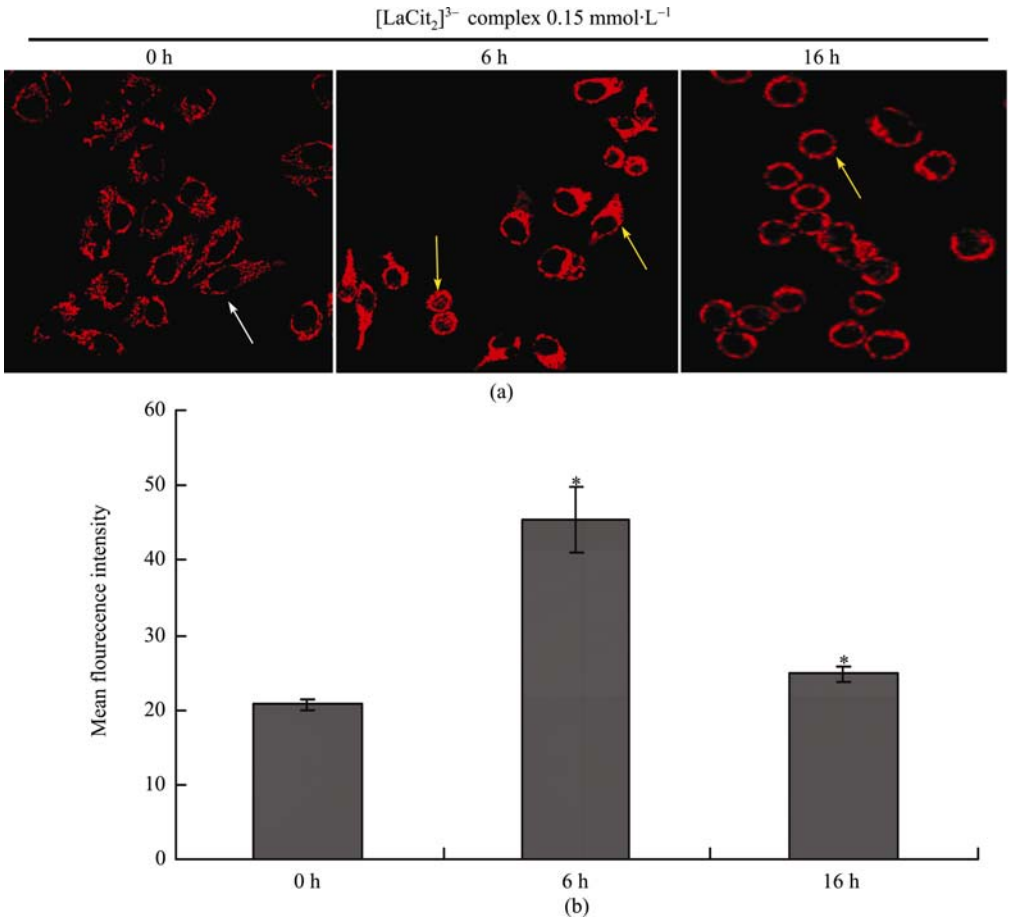

Figure 3 Effects of $[LaCit_2]^{3-}$ on the release of cyt-c in HeLa cells. (a) *In situ* distribution of cytochrome c in HeLa cells analyzed by laser scanning confocal microscopy. The white arrow indicates the representative control cell with a non-homogeneous (or clumpy) cyt-c staining pattern. The yellow arrows indicate the representative $[LaCit_2]^{3-}$-treated cells with the release of cyt-c to cytosol. (b) The fluorescent intensity of cyt-c in the cytosol quantified with confocal software. Each value represents the mean ± S.D. of three separate determinations (*$P < 0.05$ compared with the control.)

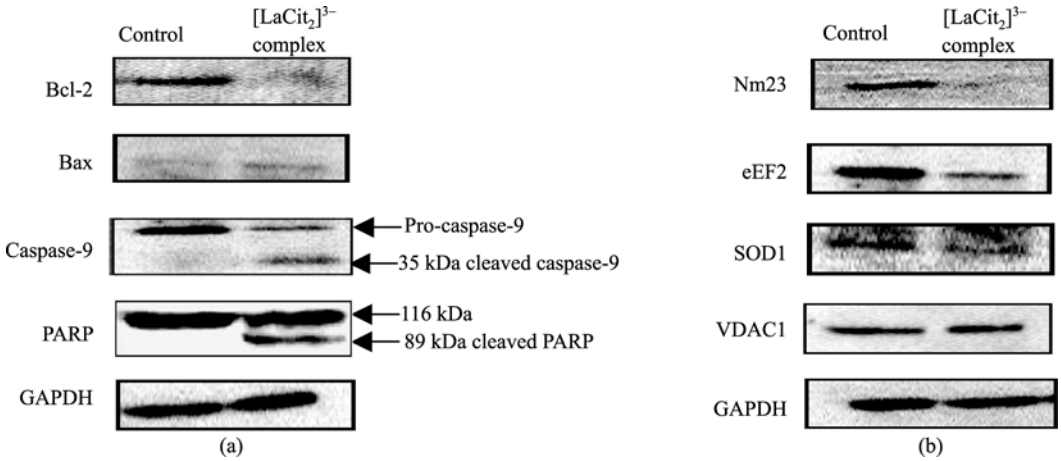

Figure 4 The $[LaCit_2]^{3-}$-sensitive proteins in HeLa cells identified by western blotting analysis. (a) Apoptosis-regulating proteins, including Bcl-2, Bax, the 37-kDa cleaved form of caspase-9 and 89-kDa cleaved PARP. (b) Western blot analysis of the altered proteins in $[LaCit_2]^{3-}$-treated HeLa cells. This is a representative result from three independent experiments. GAPDH was used as an internal control.

that the VDAC plays a key role in the regulation of MT-mediated apoptosis. In the present study, the protein VDAC2 was not detected (result not shown) and VDAC1 showed no changes in expression level (Figure 4(b)). These results suggest that VDAC expression levels might not play a key role in the process of $[LaCit_2]^{3-}$-

induced HeLa cell apoptosis, which suggests that there must be another pathway involved.

On the other hand, Ca^{2+} overload induces the opening of the PTP and appears to induce both apoptotic and necrotic cell death[18]. Ca^{2+} can regulate VDAC activity. In isolated mitochondria, Ca^{2+} induces membrane permeability transition, PTP opening and the release of cyt-c[19,20]. La^{3+} ions, as analogs to Ca^{2+} [21], could bind directly to the divalent metal binding sites on the outer side of the PTP and thus induce its opening or closing. La^{3+} might also prevent the MPT by inhibiting the accumulation of Ca^{2+} by MT[22]. La^{3+} displays a dual profile of effects towards MT, depending on the concentrations used. Exposure to La^{3+} at low concentrations (10—100 nmol·L^{-1}) induced permanent swelling, dissipation of membrane potential, ROS production, lipid peroxidation and release of cyt-c[9]. However, La^{3+} at a higher concentration induced VDAC closure when assayed in single or multichannel studies[23,24]. La^{3+} can be dissociated from $[LaCit_2]^{3-}$, and our results suggest that La^{3+} acts as a 'super calcium' with mitochondria during $[LaCit_2]^{3-}$-induced HeLa cell apoptosis, rather than as a calcium antagonist. We suspect that La^{3+} might permeate the membrane and function as Ca^{2+} to activate the PTP opening in HeLa cells.

In sum, MT dysfunction is a key event in the apoptosis induced by $[LaCit_2]^{3-}$. This is in good accordance with published data[7−9]. In addition, lanthanum complex in the form of $[LaCit_2]^{3-}$ could slowdown the formation of lanthanum phosphate precipitated in the culture medium, which is better for lanthanum to exert its biological functions during cell culture. On the contrary, free La^{3+} ion provided by its soluble salt reacts rapidly with phosphate in the culture medium, leading to the precipitation of lanthanum phosphate.

3.2 ROS generation associated with apoptosis induced by $[LaCit_2]^{3-}$

The overproduction of ROS induces oxidative stress, which is known to cause various forms of apoptosis. The release of cyt-c and consequent disruption of the electron transport chain also enhance the generation of ROS[25]. In the present study, intracellular ROS level was measured with H_2O_2 sensitive probe DCFH2-DA. H_2O_2 levels were found to be significantly higher ($P < 0.05$) in HeLa cells after 12 or 24 h treatment with $[LaCit_2]^{3-}$ (Figure 2). This result suggests that ROS induced by $[LaCit_2]^{3-}$ could be another important factor accounting for apoptosis in this model. This is consistent with previous studies[8,9] and is in agreement with observations from our proteomic analysis, which reveals profound alternations of oxidative and stress response proteins (Figure 1, Table 1). For example, SOD1, acting as a major defense against ROS by detoxifying the superoxide anion, was downregulated (Figures 1, 4(b) and Table 1). Recently, it was reported that SOD1 is localized predominantly in MT in various types of cells[26]. SOD1 and cyt-c are released simultaneously from mitochondria under the conditions when ROS generation and mitochondrial swelling take place. The release of SOD1 accelerates the accumulation of intracellular ROS and increases the susceptibility of mitochondria to oxidative stress, thereby enhancing a vicious cycle leading to apoptosis[27]. In addition, the application of SOD1 siRNA induces HeLa cell death rather than senescence[28].

3.3 Other pathways involved in $[LaCit_2]^{3-}$ cytotoxicity

During programmed cell death there is a considerable and rapid reduction in the global rate of protein synthesis[29,30]. In this study, decreased expression level of eFF2 (Figures 1, 4(b) and Table 1), RPLP0 (Figure 1, Table 1) and increased levels of the proteasome beta 3 subunit (Figure 1, Table 1) imply that $[LaCit_2]^{3-}$ induces apoptosis in HeLa cells via the translation elongation and proteasome-related pathway. This clearly needs further study.

Our results also show that the protein Nm23 (human nucleoside diphosphate kinase B complex; Figure 1, Table 1) and the nm23 protein were downregulated (Figure 4(b)). 'Nm23' is the collective designation for two closely related proteins encoded by the genes *nm23H1* and *nm23H2* (now called *NME1* and *NME2*). Nm23 gene expression is strictly related to the state of cell growth. Cells transfected with nm23 antisense RNA showed consistently slower proliferative activity than controls[31]. The ability of nm23 family of proteins to regulate a diverse set of cellular processes has recently been linked to their ability to modulate signal transduction through several growth factors, such as transforming growth factor beta 1, nerve growth factor, platelet-derived growth factor and insulin-like growth factor-1[32]. Our results suggest that the downregulation of *nm23* gene expression was related to $[LaCit_2]^{3-}$-induced apoptosis.

4 Conclusions

In the present study, 14 proteins were identified with significantly altered expression in HeLa cells with and without $[LaCit_2]^{3-}$ treatment. Most of these proteins are involved in cell apoptosis and proliferation, stress response and redox balance, protein translation and degradation. Of these proteins, the altered expressions of eEF2 and SOD1 were further confirmed by Western blotting. The mechanism study shows that $[LaCit_2]^{3-}$ treatment induced an increase in MT permeability associated with generation of H_2O_2 generation, cyt-c release, and Bax/Bcl-2 ratio alteration, leading to the activation of caspase 9 and the cleavage of PARP. Therefore, it could be concluded that $[LaCit_2]^{3-}$ induces the apoptosis of HeLa cells through oxidative stress mediated pathway involving MT participation.

We thank Drs. WANG Yong (College of Life Sciences, Shenzhen University, Shenzhen, China) and LAN Ziyao for providing help.

1 Dai Y, Li J, Li J, Yu L, Dai G, Hu A, Yuan L, Wen Z. Effects of rare earth compounds on growth and apoptosis of leukemic cell lines. In Vitro Cell Dev Biol Anim, 2002, 38: 373－375
2 Yu S, Yuan L, Yang X, Wang K, Ke Y, Qian Z M. La^{3+}-promoted proliferation is interconnected with apoptosis in NIH 3T3 cells. J Cell Biochem, 2005, 94: 508－519
3 Yu S, Hu J, Yang X, Wang K, Qian Z M. La^{3+}-induced extracellular signal-regulated kinase (ERK) signaling via a metal-sensing mechanism linking proliferation and apoptosis in NIH 3T3 cells. Biochemistry, 2006, 45: 11217－11225
4 Liu Y, Chen D, Jiang W. Anti-tumor effects of $LaCl_3$ on hepatocellular carcinoma in mice (in Chinese). J Chin Rare Earths Soc, 2008, 26: 604－608
5 Li X, Zhou A, Yu W, Chen X. Effect of lanthanum citrate on two cell lines: human lung cancer cells PG and human gastric carcinoma cells BGC-823 (in Chinese). J Chin Rare Earths Soc, 2000, 18: 156－158
6 Meyers C A, Smith J A, Bezjak A, Mehta M P, Liebmann J, Illidge T, Kunkler I, Caudrelier J M, Eisenberg P D, Meerwaldt J, Siemers R, Carrie C, Gaspar L E, Curran W, Phan S C, Miller R A, Renschler M F. Neurocognitive function and progression in patients with brain metastases treated with whole-brain radiation and motexafin gadolinium: results of a randomized phase III trial. J Clin Onco, 2004, l22: 157－65
7 Heffeter P, Jakupec M A, Körner W, Wild S, von Keyserlingk N G, Elbling L, Zorbas H, Korynevska A, Knasmüller S, Sutterlüty H, Micksche M, Keppler B K, Berger W. Anticancer activity of the lanthanum compound [tris(1,10-phenanthroline) lanthanum(Ⅲ)] trithiocyanate (KP772; FFC24). Biochem Pharmacol, 2006,71: 426－40
8 Liu H, Yuan L, Yang X, Wang K. La^{3+}, Gd^{3+}, and Yb^{3+} induced changes in mitochondrial structure, membrane permeability, cytochrome c release and intracellular ROS level. Chem-Biol Interact, 2003, 146: 27－37
9 Dong S, Zhao Y, Liu H, Yang X, Wang K. Duality of effect of La^{3+} on mitochondrial permeability transition pore depending on the concentration. BioMetals, 2009, DOI10.1007/s10534-009-9244-1
10 Yu S, Hu J, Yang X, Wang K, Qian Z M. La^{3+}-induced extracellular signalregulated kinase (ERK) signaling via a metal-sensing mechanism linking proliferation and apoptosis in NIH 3T3 cells. Biochemistry, 2006, 45: 11217－11225
11 Wang Z M, Lin H K, Zhu S R, Liu T F, Zhou Z F, Chen Y T. Synthesis, characterization and cytotoxicity of lanthanum (Ⅲ) complexes with novel 1, 10-phenanthroline-2, 9-bis-alpha-amino acid conjugates. Anticancer Drug Des1, 2000, 5: 405－11
12 Wang Z M, Lin H K, Zhu S R, Liu T F, Chen Y T. Spectroscopy, cytotoxicity and DNA-binding of the lanthanum (Ⅲ) complex of an L-valine derivative of 1-10-phen-anthroline. J Inorg Biochem, 2002, 89: 97－106
13 Shen L M, Lan Z Y, Liu Q, Ni J Z. Apoptosis of cancer cells induced by lanthanum citrate (in Chinese). J Chin Rare Earths Soc, 2009, 27: 441－446
14 Shen L M, Liu Q, Ni J Z, Hong G Y. A proteomic investigation into the human cervical cancer cell line HeLa treated with dicitratoytterbium (Ⅲ) complex. Chem Biol Interact, 2009, doi:10.1016/j.cbi.2009.07.013.
15 Crompton M. The mitochondrial permeability transition pore and its role in cell death. Biochem J, 1999, 341: 233－249
16 Gogvadze V, Robertson J D, Zhivotovsky B, Orrenius S. Cytochrome c release occurs via Ca^{2+}-dependent and Ca^{2+}-independent mechanisms that are regulated by Bax. J Biol Chem, 2001, 276: 19066－19071
17 Neuzil J, Wang X F, Dong L F, Low P, Ralph S J. Molecular mechanism of 'mitocan'-induced apoptosis in cancer cells epitomizes the multiple roles of reactive oxygen species and Bcl-2 family proteins. FEBS Letters, 2006, 580: 5125－5129
18 Tsujimoto Y, Shimizu S. Role of the mitochondrial membrane permeability transition in cell death. Apoptosis, 2007, 12: 835－840
19 Duchen M R, McGuinness O, Brown L A, Crompton M. On the involvement of a cyclosporin A sensitive mitochondrial pore in myocardial reperfusion injury. Cardiovasc Res, 1993, 27: 1790－1794
20 Imberti R, Nieminen A L, Herman B, Lemasters J J. Mitochondrial and glycolytic dysfunction in lethal injury to hepatocytes by t-butylhydroperoxide: protection by fructose, cyclosporin A and trifluoperazine. J Pharmacol Exp Ther, 1993, 265: 392－400
21 Ni J Z. Bioinorganic Chemistry of Rare Earth Elements. Beijing: Science Press, 1995. 13－59
22 Mela L. Interactions of La^{3+} and local anesthetic drugs with mitochondrial $Ca^{2+}$and Mn^{2+} uptake. Arch Biochem Biophys, 1968, 123: 286－293
23 Gincel D, Zaid H, Shoshan-Barmatz V. Calcium binding and translocation by the voltage-dependent anion channel: a possible regulatory mechanism in mitochondrial function. Biochem J, 2001, 35: 147－155
24 Shoshan-Barmatz V, Gincel D. The voltage-dependent anion channel: characterization, modulation, and role in mitochondrial function in cell life and death. Cell Biochem Biophys, 2003, 39: 279－292
25 Cai J, Jones D P. Superoxide in apoptosis: mitochondrial generation triggered by cytochrome c loss. J Biol Chem, 1998, 273: 11401－11404
26 Kira Y, Sato E F, Inoue M. Association of Cu, Zn-type superoxide dismutase with mitochondria and peroxisomes. Arch Biochem Biophys, 2002, 399: 96－102
27 Li Q, Sato E F, Zhu X, Inoue M. A simultaneous release of SOD1 with cytochrome c regulates mitochondria-dependent apoptosis. Mol Cell Biochem, 2008, 322: 151－159
28 Blander G,de Oliveira RM,Conboy C M, Haigis M,Guarente L. Superoxide dismutase 1 knock-down induces senescence in human fibroblasts. J Biol Chem, 2003, 278(40): 38966－9
29 Clemens M J, Bushell M, Morley S J. Degradation of eukaryotic polypeptide chain initiation factor (eIF) 4G in response to induction of apoptosis in human lymphoma cell lines. Oncogene, 1998, 17: 2921－2931
30 Morley S J, McKendrick L, Bushell M. Cleavage of translation initiation factor 4G (eIF4G) during anti-Fas IgM-induced apoptosis does not require signalling through the p38 mitogen-activated protein (MAP) kinase. FEBS Lett, 1998, 438: 41－48
31 Cipollini G, Berti A, Fiore L, Rainaldi G, Basolo F, Merlo G, Bevilacqua G, Caligo M A. Down-regulation of the nm23.h1 gene inhibits cell proliferation. Int J Cancer, 1997, 73(2): 297－302
32 Otero A S. NM23/nucleoside diphosphate kinase and signal transduction. J Bioenerg Biomembr, 2000, 32: 269－275